1 **Strain specific persistence in the murine lung of *Aspergillus fumigatus* conidia**

2 **causes an Allergic Broncho-Pulmonary Aspergillosis-like disease phenotype**

3

4 Jane T. Jones[1], Ko-Wei Liu[1], Xi Wang[1], Caitlin H. Kowalski[1], Brandon S. Ross[1],

5 Kathleen A. M. Mills[2,3], Joshua D. Kerkaert[1], Tobias M. Hohl[2,3], Lotus A. Lofgren[4], Jason

6 E. Stajich[4], Joshua J. Obar[1], and Robert A. Cramer[1]

7

8 [1]Geisel School of Medicine, and Department of Microbiology and Immunology,

9 Dartmouth, Hanover, NH 03755 USA

10 [2]Infectious Disease Service, Department of Medicine, Memorial Sloan Kettering Cancer
11 Center, New York, NY, USA
12
13 [3]Immunology and Microbial Pathogenesis Graduate Program, Weill Cornell Graduate
14 School, New York, NY, USA

15 [4]Department of Microbiology and Plant Pathology, University of California Riverside,

16 Riverside, CA 92507 USA

17

18

19 Corresponding Author:

20 Robert A. Cramer, Ph.D.; robert.a.cramer.jr@dartmouth.edu

21

24

1

25   ABSTRACT

26   *Aspergillus fumigatus* is a filamentous fungus which can cause multiple diseases

27   in humans. Allergic Broncho-pulmonary Aspergillosis (ABPA) is a disease diagnosed

28   primarily in Cystic Fibrosis patients caused by a severe allergic response often to long-

29   term *A. fumigatus* colonization in the lungs. Mice develop an allergic response to

30   repeated inhalation of *A. fumigatus* spores; however, no strains have been identified

31   that can survive long-term in the mouse lung and cause ABPA-like disease. We

32   characterized *A. fumigatus* strain W72310 by whole genome sequencing and *in vitro*

33   and *in vivo* viability assays in comparison to a common reference strain, CEA10.

34   W72310 was resistant to leukocyte-mediated killing and persisted in the mouse lung

35   longer than CEA10, a phenotype that correlated with greater resistance to oxidative

36   stressors, hydrogen peroxide and menadione, *in vitro*. In animals both sensitized and

37   challenged with W72310, conidia, but not hyphae, were viable in the lungs for up to 21

38   days in association with eosinophilic airway inflammation, airway leakage, serum IgE,

39   and mucus production. W72310-sensitized mice that were recall-challenged with

40   conidia had increased inflammation, Th1 and Th2 cytokines, and airway leakage

41   compared to controls. Collectively, our studies demonstrate that a unique strain of *A.*

42   *fumigatus* resistant to leukocyte killing can persist in the mouse lung in conidial form

43   and elicit features of ABPA-like disease.

44

45   IMPORTANCE

46   Allergic Broncho-pulmonary Aspergillosis (ABPA) patients often present with long-term

47   colonization of *Aspergillus fumigatus*. Current understanding of ABPA pathogenesis has

2

48   been complicated by a lack of long-term *in vivo* fungal persistence models. We have

49   identified a clinical isolate of *A. fumigatus*, W72310, which persists in the murine lung

50   and causes an ABPA-like disease phenotype. Surprisingly, while viable, W72310

51   showed little to no growth beyond the conidial stage in the lung. This indicates that it is

52   possible that *A. fumigatus* can cause allergic disease in the lung without any significant

53   hyphal growth. The identification of this strain of *A. fumigatus* can not only be used to

54   better understand disease pathogenesis of ABPA and potential anti-fungal treatments,

55   but also to identify features of fungal strains that drive long-term fungal persistence in

56   the lung. Consequently, these observations are a step toward helping resolve the long-

57   standing question when to utilize antifungal therapies in patients with ABPA and fungal

58   allergic type diseases.

59

60   INTRODUCTION

61   Individuals with atopic asthma, COPD, and particularly Cystic Fibrosis (CF) are

62   susceptible to chronic fungal colonization and infections in the lung (1). For example,

63   30-80% of CF patients persistently test positive for growth of the filamentous fungus,

64   *Aspergillus fumigatus,* in expectorated sputum (2–4) and this finding is associated with

65   overall decreased lung function (5). These findings demonstrate that *A. fumigatus*

66   colonization is a critical aspect of CF disease pathogenesis. A subset of these patients

67   develops Allergic Broncho-pulmonary Aspergillosis (ABPA), a particularly difficult

68   disease to diagnose and treat. Individuals with ABPA exhibit a type 2 immune response

69   that leads to the production of high levels of IL-4, airway eosinophilia, and increased

70   total and *A. fumigatus* specific IgE (6, 7). Recurrent ABPA exacerbations lead to the

3

71   development of bronchiectasis, airway remodeling, and fibrosis as a long-term

72   consequence of fungal colonization (8). Although treating ABPA patients with anti-fungal

73   drugs can improve symptoms in some cases (9, 10) it is not known how or whether

74   persistence of *A. fumigatus* in the lungs specifically contributes to ABPA disease

75   pathogenesis.

76   Murine models of fungal persistence using agar beads conjugated to *A.*

77   *fumigatus* conidia successfully recapitulated long term (21 to 28 days) colonization of

78   fungal hyphae in the lung (11, 12), however, mice in this specific agar bead model do

79   not develop the strong IgE/Th2 response observed in ABPA patients. Numerous other

80   mouse models that seek to recapitulate human ABPA have been described, including

81   utilizing *A. fumigatus* antigens (13) and repeated challenge with live conidia (14), though

82   none of these models exhibited long-term persistence of *A. fumigatus* in the airways, a

83   common and important feature of ABPA (5, 15, 16). Importantly, the extent of fungal

84   growth in ABPA patients' airways is unclear, though hyphae have been identified in

85   sputum and tissue in some patient samples (17, 18). Consequently, *in vivo* studies

86   examining the fungal contribution to ABPA development, persistence, and disease

87   progression are currently difficult to conduct. This is a critical question to address

88   because it is expected to help inform when antifungal therapies may be effective in the

89   context of ABPA.

90   The goal of the current study was to identify a strain of *A. fumigatus* that is

91   capable of long-term persistence in the lung of immune competent mice. Using a clinical

92   strain isolated from a sputum sample, viable *A. fumigatus* was recovered from the

93   murine airways for up to 21 days. Animals with persistent fungal burden developed

4

94   increased serum IgE, eosinophilia, airway damage, mucus production, and an

95   increased immune response to re-exposure to fungi, all common features of ABPA.

96   Surprisingly, these symptoms developed despite little to no hyphal growth observed in

97   the airways of animals with persistent fungal burden. Consequently, these data

98   demonstrate that a fungal strain with resistance to leukocyte killing and relatively low

99   virulence is capable of long-term persistence in the murine lung and initiating ABPA-like

100   disease pathogenesis.

101

102   MATERIALS AND METHODS

103   *Animal Inoculations*: Mice were housed in autoclaved cages at $\leq$4 mice per cage with

104   HEPA-filtered air and water. For single-exposure studies, outbred Wild Type C57Bl/6

105   female mice 8-12 weeks old (Jackson Laboratories) were intranasally inoculated with

106   1×10^7 live conidia (in 40µl PBS) per mouse. *A. fumigatus* strains CEA10 and W72310

107   were grown on 1% glucose minimal media (GMM) for 3 days at 37°C, conidia were

108   collected in 0.01% Tween and washed 3 times in sterile PBS. Animals were inoculated

109   with 3×10^7 live conidia for 36 hours (FLARE), 1×10^7 live conidia 1X in week one and

110   5X in week two (sensitization), and 1×10^7 live conidia on the first day of week three

111   (challenge). Animals were monitored daily for disease symptoms and we carried out our

112   animal studies in strict accordance with the recommendations in the *Guide for the Care*

113   *and Use of Laboratory Animals*. The animal experimental protocol 00002241 was

114   approved by the Institutional Animal Care and Use Committee (IACUC) at Dartmouth

115   College.

116   *Hygromycin-resistant and mRFP strain generation:* Protoplasts from strains CEA10 and

117   W72310 were generated with *Trichoderma harzianum* (Millipore Sigma) lysing enzyme

118   and transformed ectopically with linear constructs of *gpdA*-driven *hph* hygromycin-

119   resistance gene or H2A:mRFP (CEA10) as previously described (19, 20).

120   *RNA preparation and NanoString Analysis:* Animals were "sensitized" to either PBS,

121   CEA10, or W72310 as described previously and lungs were removed at euthanasia for

122   mRNA analysis. Lungs were freeze dried, homogenized with glass beads using Mini

123   Bead Beater (BioSpec Products Inc, Bartlesville, OK) and resuspended in Trizol

124   (Thomas Scientific) and chloroform to extract RNA according to manufacturer's

125   instructions. After RNA was assessed for quality, 500ng of RNA was used per

126   NanoString reaction using the nCounter Mouse Immunology v1 Gene Expression Panel

127   (NanoString). nSolver 4.0 software was used for background subtraction and

128   normalization. nCounter Advanced Analysis 2.0 was used for quality control analysis

129   and pathway analysis. For additional pathway analysis, accession numbers were

130   converted to Entrez IDs via the DAVID Gene Accession Conversion Tool (21, 22). The

131   Entrez IDs were then used to pull GO terms for each gene from the Mouse Genome

132   Informatics' website (http://www.informatics.jax.org/batch). The resulting file was

133   reformatted to fit the TopGO package's requirements for gene ID to GO ID conversion

134   (gene_ID \t GOID1;GOID2;...;GOIDX). Genes were classified as increased or

135   decreased based on a 2-fold change cutoff and a p-value $\leq$ 0.05. Lists of all differentially

136   expressed genes (DEGs), increased DEGs, or decreased DEGs were inserted into

137   separate TopGOdata objects using the gene ID to GO ID conversion file to assign all

138   possible GO terms for each gene. A nodesize cutoff of 10 was used and a Classic

139   Fischer's test followed by a Benjamini-Hochberg correction for multiple testing was

140   performed via the TopGO R package (23) to determine enriched GO terms within the

141   datasets. The degree of enrichment was calculated as the number of significant genes

142   divided by the number of genes expected by random chance. Data was plotted via the

143   ggplot2 and ComplexHeatmap (24) packages in R version 3.6.2 (2019-12-12).

144   *Colony Forming Units:* Whole lungs were homogenized in 1ml sterile PBS using glass

145   beads in a Mini Bead beater. Serial dilutions (1:10-1:1000) were then spread onto agar

146   plates containing Sabouraud media or Sabouraud media containing 175µg/ml

147   hygromycin and incubated O/N at 37°C. Plate dilutions containing 50-100 visible

148   colonies were quantified and expressed as a measurement of Colony Forming Units per

149   ml (CFUs/ml).

150   *Histology: GMS, PAS, H&E:* After euthanasia, cannulas were inserted into trachea and

151   lungs were excised from the body cavity. Lungs were inflated with 10% buffered

152   formalin phosphate for 24h and stored in 70% ethanol until embedding. Paraffin-

153   embedded sections were stained with hematoxylin and eosin (H&E), Grocott-Gomori

154   methenamine silver (GMS), and Periodic Acid Schiff (PAS). Slides were analyzed

155   microscopically with a Zeiss Axioplan 2 imaging microscope (Carl Zeiss Microimaging,

156   Inc., Thornwood, NY) fitted with a QImaging Retiga-SRV Fast 1394 RGB camera.

157   *Serum Analysis:* Cardiac punctures were performed post-mortem. After 1 hr at room

158   temperature, blood samples were centrifuged at 2000g for 30 minutes and serum was

159   isolated. Total IgE was measured by ELISA using kit (Invitrogen) and performed

160   according to manufacturer's instructions.

7

161 *Broncho-Alveolar Lavage (BAL) Analysis (inflammatory cells, Albumin, ELISAs):* After

162 euthanasia, cannulas were inserted into trachea and lungs were removed. Lungs were

163 lavaged with 3 sequential cold PBS washes (1ml, 0.5ml, 0.5ml). BAL was centrifuged at

164 300g for 5 minutes and supernatant was removed for cytokine (IL-4, IL-10, and IFNγ

165 R&D) and albumin (Eagle Diagnostics) analysis according to manufacturer's

166 instructions. Remaining cells were counted and centrifuged onto slides using Rotofix

167 Cytospin. Up to 300 cells were counted to determine percentages of macrophages,

168 neutrophils, eosinophils, and lymphocytes. Total numbers of individual cell populations

169 were calculated using individual percentages multiplied by total BAL cell numbers.

170 *Cell Death Assay*: L-GMM was inoculated with 2.0 X 10^6 mRFP-CEA10 or mRFP-

171 W72310 and incubated with either 25μM menadione or 5mM hydrogen peroxide for 6 hr

172 at 37°C. After incubation, conidia were run on Beckman Coulter Cytoflex S Flow

173 Cytometer for % positive RFP (viability). Analysis was performed using FlowJo version

174 9.9.6 as previously described (25).

175 *Isolation of Bone Marrow and Co-Culture Conditions*: After euthanasia, femur and tibia

176 were extracted from 8-12 week old C57Bl/6 mice and the bones were flushed with PBS

177 to collect bone marrow-derived cells. After red blood cell lysis, cells were counted and

178 cultured with either mRFP-CEA10 or mRFP-W72310 AF633-stained conidia as

179 described (Jhingran et al. 2012) for 16h 10:1 MOI with 10 ng/ml interferon gamma

180 (IFNγ) and 25mM hydroxyurea (HU).

181 *Flow Cytometry and Fluorescence Aspergillus REporter (FLARE) Analysis*: Whole lung

182 single cell suspensions were prepared as described (20). Briefly, lungs were minced

8

183 and digested in buffer containing 2.2 mg/ml collagenase type IV (Worthington),

184 100µg/ml DNase I (Zymo Research) and 5% FBS at 37°C rotating for 45 minutes.

185 Digested samples were then passed through an 18 gauge needle, resuspended in Red

186 Blood Cell lysis buffer, diluted with PBS, passed through a 100µm filter, and counted.

187 For flow cytometry analysis, cells were stained with a viability dye (eFluor 780,

188 eBioScience), anti-CD45 (Pacific Orange, Invitrogen), anti-CD11b (PECy5, BioLegend

189 for cellularity, PerCPCy5.5, BioLegend for FLARE), anti-CD11c (PE, BioLegend), anti-

190 Ly6G (FITC, BioLegend), anti-CD64 (BV421, BioLegend) and anti-SiglecF (BV421, BD

191 bioscience). Samples were analyzed on a MacsQuant VYB flow-cytometer (cellularity)

192 or Beckman Coulter Cytoflex S (FLARE). Macrophages were identified as CD45$^+$/Ly6G$^-$

193 /CD11b$^+$/CD64$^+$, neutrophils were identified as CD45$^+$/SiglecF$^-$/Ly6G$^+$/CD11b$^+$ and

194 eosinophils were identified as CD45$^+$/SiglecF$^+$/CD11c^{low}. Analysis was performed with

195 FlowJo version 9.9.6.

196 *Genome Sequencing and Variant Analyses:* Mycelial cultures of *A. fumigatus* using

197 liquid glucose minimal media with yeast extract were inoculated in small petri dishes

198 grown overnight (18-24hrs) at 37C. Mycelia were collected, lyophilized, and bead

199 beaten to powder and DNA was extracted as previously described (27). Genomic

200 sequencing libraries of the DNA were constructed using the SeqOnce (SeqOnce

201 Biosciences, Pasadena, CA) with multiplexing barcodes by the Genomics Core at UC

202 Riverside Institute for Integrative Genome Biology. The genomic libraries were

203 sequenced as 2 x 150 bp reads on Illumina Novaseq 6000 (Illumina, San Diego, CA) at

204 UC San Francisco Sequencing Core to generate ~2.17 Gb of sequence. Sequence data

205 for W72310 was deposited in the Sequence Read Archive under BioProject

9

206 PRJNA614926. Sequence data for strain CEA10 was obtained from Sequence Read

207 Archive under accession ERR232423 and BioProject PRJEB1497. The sequence reads

208 for each strain were aligned to the Af293 genome downloaded from FungiDB v.46 (28,

209 29) using BWA v0.7.17 (30) and converted to the BAM file format after running fixmate

210 and sort commands in samtools v1.10 (Li et al., 2009). Duplicate reads were removed

211 and reads indexed using MarkDuplicates and Build BamIndex in picard tools v2.18.3

212 (http://broadinstitute.github.io/picard). To avoid overcalling variants near alignment

213 gaps, reads were further realigned using RealignerTargetCreator and IndelRealigner in

214 the Genome Analysis Toolkit GATK v3.7 (Auwera et al., 2013). The variants (SNPs and

215 INDELS) for W72310 and CEA10 were genotyped relative to the *A. fumigatus* reference

216 genome Af293 using HaplotypeCaller step in GATK v4.0 (doi: 10.1101/201178).

217 Filtering was accomplished using GATK's SelectVariants call with the following

218 parameters: for SNPS: -window-size = 10, -QualByDept < 2.0, -MapQual < 40.0, -

219 QScore < 100, -MapQualityRankSum < -12.5, -StrandOddsRatio > 3.0, -

220 FisherStrandBias > 60.0, -ReadPosRankSum < -8.0. For INDELS: -window-size = 10, -

221 QualByDepth< 2.0, -MapQualityRankSum < -12.5, -StrandOddsRatio > 4.0, -

222 FisherStrandBias > 200.0, -ReadPosRank < -20.0 , -InbreedingCoeff < -0.8. Resultant

223 variants were annotated with snpEff (Cingolani et al., 2012) using the Gene File Format

224 gene annotation for Af293 v.46 in FungiDB. Variants that overlapped transposable

225 elements (TEs) were removed by positional mapping to locations of annotated TEs in

226 the FungiDB v.46 release of the Af293 reference genome, using BEDtools -subtract

227 (Quinlan and Hall, 2010). Mutations in W72310 were analyzed relative to CEA10 using

228 a custom script implemented in the R programing environment (R core team 2013). To

229   identify mutations occurring in allergen genes, a database of genes putatively capable

230   of eliciting immune response was curated from the published literature (n = 113) (Table

231   2) and mapped against W72310 variant positions using a custom script in R. Putative

232   allergen genes in W72310 containing variants other than synonymous or intergenic

233   mutations were annotated in Fungi DB v.46 (29). To investigate variants unique to

234   W72310 and occurring in genes relevant to the phenotypes of interest in this study

235   (oxidative stress, cell wall integrity, primary metabolism, and melanin production), we

236   used reverse GO mapping of the terms GO: 0006979 (response to oxidative stress),

237   GO:0005618 (cell wall), GO:0044238 (primary metabolic process) GO:0006582

238   (melanin metabolic process) and GO:0042438 (melanin biosynthetic process). The code

239   and datafiles for variant assessment associated with this project can be accessed via

240   GitHub in the repository: stajichlab/W72310 (DOI: 10.5281/zenodo.4116457)(31).

241   *Statistical Analysis:* All statistical analyses were performed with Prism 8.3 software

242   (GraphPad Software Inc., San Diego, CA). For *in vitro* comparison of 2 groups,

243   Student's T-test was used. For animal experiments, nonparametric analyses were

244   performed (Kruskal-Wallis, Dunn's multiple comparisons; Mann-Whitney, single

245   comparisons). All error bars represent standard errors of the means. NS $P>0.05$; *

246    $P \leq 0.05$; ** $P \leq 0.01$; *** $P \leq 0.001$; **** $P \leq 0.0001$.

247

248   RESULTS

249   *Aspergillus fumigatus clinical isolate, W72310, is resistant to immune cell-mediated*

250   *killing and persists in the murine lung:* Previous work from our laboratory found that a

251   clinical isolate strain, W72310, had reduced virulence compared to the commonly

252   studied reference strain, CEA10, in mice with suppressed immune systems (32).

253   Conidia from W72310 have also been reported to germinate more slowly under a

254   variety of conditions (33) in comparison to other *A. fumigatus* strains. We hypothesized

255   that a slow growing, less virulent strain may evade immune clearance and allow

256   establishment of long-term fungal persistence in murine airways. In order to test this

257   hypothesis, we first compared W72310 and CEA10 persistence in the immune

258   competent murine lung 7 days after one fungal intranasal inoculation. GMS staining of

259   fixed lungs revealed that fungal conidia were still present in W72310-exposed lungs 7

260   days post inoculation, however, no observable conidia were found in CEA10 challenged

261   animals (Fig. 1A). While swollen conidia could be observed in W72310 inoculated

262   animals, no hyphal growth was visible across multiple independent histopathology

263   sections. In a parallel experiment, quantification of total colony forming units revealed

264   viable fungi only from lungs inoculated with W72310 (Fig 1B), indicating W72310

265   persists longer than CEA10 in C57BL6/J mice.

266   To address how W72310 conidia persist in the lung, we assayed the

267   susceptibility of W72310 and CEA10 fungal conidia to killing by bone marrow-derived

268   neutrophils and macrophages *ex vivo*. CEA10 and W72310 that ectopically express

269   mRFP were generated in order to distinguish live (mRFP$^+$) from dead (mRFP$^-$) conidia

270   by flow cytometry. Given the relatively short half live of RFP (approximately 45 minutes)

271   in the phagolysosome of leukocytes, this fluorescent protein functioned as a fungal

272   viability marker during cellular interactions with leukocytes. A fluorescent tracer dye

273   (Alexa Fluor 633) was covalently attached to the surface of the mRFP-expressing

12

274   strains and served as a conidial tracer (26). After co-culture of either mRFP-

275   W72310/AF633 or mRFP-CEA10/AF633 conidia and bone marrow cells for 16 h, there

276   were 15% more neutrophils positive for CEA10 conidia compared to W72310 conidia,

277   while there were no differences observed in macrophages (Supp fig. S1A). A small but

278   significant increase in survival of W72310 was observed in neutrophils compared to

279   CEA10. The survival of W72310 conidia was higher by 15% compared to CEA10 in

280   macrophages (Supp fig. S1B). To test this observation *in vivo*, we utilized the FLARE

281   assay to quantify leukocyte uptake and viability of W72310 and CEA10 conidia in the

282   murine lung. 36 hr after inoculation with AF633-stained mRFP-CEA10 or W72310

283   conidia, the percentage of W72310 conidia that were phagocytosed by CD45^{+} immune

284   cells was 30% less than the percentage of CEA10 conidia in CD45^{+} immune cells (Fig.

285   1C). However, comparison of neutrophil and macrophage conidial uptake (% positive

286   AF633) showed no difference between CEA10 and W72310 (Fig. 1D), in contrast to

287   observations in the bone marrow-derived neutrophils. The reduced phagocytosis of

288   W72310 conidia correlated with a four-fold reduction in neutrophils and two-fold

289   reduction in total macrophages in the lungs of mice inoculated with W72310 compared

290   to CEA10 (Fig. 1E). The percentage of viable W72310 conidia phagocytosed by

291   neutrophils and macrophages significantly increased four-fold in comparison to CEA10

292   (Fig. 1F and G). Taken together, these data suggest the *A. fumigatus* strain W72310

293   recruits less inflammatory cells and is killed less efficiently than the highly virulent

294   CEA10 strain in a murine model of fungal bronchopneumonia.

295   *Comparison of W72310 sensitization to CEA10 sensitization in the murine lung*: Given

296   the persistent presence of the W72310 strain in the murine lung, its increased

297 resistance to leukocyte-mediated killing, and the altered cellular response to W72310

298 conidia, we next compared the overall immune response to sensitization with CEA10

299 and W72310 live conidia. Animals were intranasally inoculated and sensitized to

300 W72310 or CEA10 conidia as indicated (Fig. 2A). Compared to PBS-sensitized animals,

301 CEA10 and W72310 animals had 6- and 8-fold increased serum IgE, respectively (Fig.

302 2B). Although we observed a trend for more total IgE in animals exposed to W72310

303 compared to CEA10, the difference was not statistically significant. Additionally, small

304 but detectable CFUs were observed in lungs sensitized with CEA10, however,

305 approximately 10^6 CFUs were detected in lungs of animals sensitized with W72310

306 (Fig. 2C). In parallel, total RNA was extracted from whole lungs and analyzed for

307 changes in mRNA levels of immune-related genes using NanoString nCounter

308 technology. As expected, overall changes in mRNA levels were strikingly different in

309 PBS-sensitized animals compared to the two fungal strains (Fig. 2D). Increased

310 signatures in pathways related to cytokine/chemokine signaling, host pathogen

311 interactions, and innate and adaptive immune signaling were observed in fungal

312 challenged animals as expected (Fig. 2E.). Interestingly, the only immune-related

313 pathways with reduced mRNA levels in fungal-exposed mice compared to PBS were

314 TGF-β and inflammasome encoding genes (Fig. 2E). Using GO-term analysis with a

315 cut-off of $P \leq 0.01$ to differentiate highly significant pathways in the W72310-sensitized

316 lung compared to PBS, analysis showed prevalent eosinophil, monocyte, and

317 lymphocyte chemotaxis, ERK1 and ERK2 signaling, IFNγ-response signaling, and

318 general immune system responses (Fig. 2F). Comparison of PBS and W72310-

319 sensitized lungs revealed 174 increased and 38 decreased mRNA transcripts (Fig. 2G).

14

320   Surprisingly, transcripts of only 9 genes were differentially abundant (2-fold or higher)

321   between CEA10 and W72310 challenged mice. Of these, transcripts of all 9 genes were

322   increased in W72310 sensitized animals compared to CEA10 sensitized animals (Fig.

323   2H). These differentially expressed transcripts are encoded by the genes *nos2, clec4e,*

324   *cxcl-9, cxcl-10, ccl4, cxcl-11, klra21, cxcl3, and tnfα*; transcripts largely involved in T

325   cell/monocyte recruitment and activation, host defense, and CXCR3 receptor activation.

326   The lack of differences between CEA10 and W72310 challenged animals seems

327   especially striking given the clear differences in persistent fungal burden.

328   *W72310 accumulates in the murine lung during sensitization*: ABPA patients are

329   sensitized to *A. fumigatus* antigens (34). A previous report demonstrated that fungi

330   could persist longer in an allergen-sensitized murine lung compared to a control lung

331   (35), so we next determined whether sensitization with W72310 or CEA10 increased

332   persistence of a subsequent exposure to W72310 or CEA10 conidia. In light of the data

333   from the immune competent murine model (Fig. 1), it is likely that W72310 sensitization

334   alone would cause an accumulation of fungi in the lung, so in order to differentiate

335   between fungi present from sensitization and fungi present due to challenge, we

336   generated CEA10 and W72310 strains that were resistant to hygromycin. Mice were

337   sensitized with either PBS, WT CEA10 or WT W72310 and challenged with either PBS,

338   W72310-hyg or CEA10-hyg. Colony forming units were measured on Sabouraud

339   Dextrose Agar (SAB)-containing plates (total CFUs) or SAB/hygromycin-containing

340   plates ("challenge" CFUs) from the lungs of mice euthanized 7 days after challenge

341   (Fig. 3A). Interestingly, no live conidia were detected in mice sensitized with CEA10 and

342   challenged with PBS, demonstrating that repeated intranasal (IN) inoculation was not

15

343   sufficient to drive CEA10 fungal conidia accumulation in the murine lung (Fig. 3B). In

344   contrast, approximately 1×10^7 live conidia were detected from mice sensitized with

345   W72310 and challenged with PBS, indicating an accumulation of viable fungi in the lung

346   from repeated W72310 IN sensitizations (Fig. 3B). Challenge with CEA10-hyg in

347   W72310-senstized mice did not facilitate persistence of CEA10, however, an almost

348   two-fold increase in CFUs was observed in W72310-challenged mice when sensitized

349   with W72310 but not CEA10 (Fig. 3B). Collectively these data indicate that sensitization

350   causes a modest increase in persistence of W72310 but not CEA10. Consequently,

351   fungal sensitization itself is not sufficient nor necessary to promote fungal persistence in

352   the lung with all strains of *A. fumigatus.*

353   *Sensitization and Challenge with W72310 causes increased fungal persistence in the*

354   *lung in association with increased serum IgE:* To determine whether W72310 persists

355   long-term in the mouse lung, we sensitized animals as described in Figure 2 and

356   subsequently "challenged" mice with another fungal dose on day 0 (Fig. 4A). As a

357   control, animals were sensitized to PBS only and challenged with one dose of W72310

358   on day 0. To determine fungal persistence, CFUs were chosen for quantitation despite

359   the filamentous morphology of *A. fumigatus* because hyphal elements could not be

360   observed in histopathology samples at any time point. Total CFUs increased in the

361   lungs of animals sensitized and challenged with W72310 at 2, 7, and 21 days post

362   challenge in comparison to PBS-sensitized controls (Fig. 4B). This significance was not

363   observed in lungs 28 days post challenge. CFUs were detected 2 and 7 days post

364   challenge in the PBS sensitized control group. Surprisingly, CFUs were still detectable

365   21 and 28 days post challenge in this group as well, although to a much lesser extent.

366 Fixed lungs were stained for fungi (GMS) to observe the fungal presence and

367 morphology. At 2 and 7 days post challenge in both PBS and W72310-sensitized mice,

368 prominent conidia were visible (Fig. 4C). Despite the quantification of detectable CFUs

369 in PBS-sensitized mice 21 and 28 days post challenge, conidia were not visible by GMS

370 stain (Fig. 4C). Conidia were strongly visible 21 days after challenge in the W72310-

371 sensitized mice, however, they appeared to be taken up in large vacuolar phagocytes

372 (Fig. 4C). Interestingly, multiple conidia were visible in a single host cell. Conidia were

373 mostly non-detectable by 28 days, with a small number visible by GMS stain.

374 Collectively these data demonstrate that W72310 can persist in a fungal sensitized

375 murine lung up to one month after inoculation.

376   Blood was collected from each animal and total serum IgE levels were measured

377 by ELISA to determine the overall allergic response. As expected, total IgE levels

378 increased 2 and 7 days post challenge in W72310 sensitized mice compared to controls

379 (Fig. 4D), however significant increases were not detected at 21 and 28 days.

380 Interestingly, even in the PBS-sensitized animals, total serum IgE was increased at 21

381 days compared to PBS-sensitized control at 2 days. Overall, these data indicate that

382 sensitization and challenge with strain W72310 maintain high levels of IgE.

383   *Sensitization and Challenge with W72310 causes increased inflammation,*

384 *leakage, and mucous cell metaplasia:* Eosinophilia is a hallmark of ABPA disease (36).

385 Differential staining of airway/bronchoalveolar lavage cells revealed that eosinophils

386 were increased 2, 7, and 21 days after sensitization and challenge with W72310 live

387 conidia in comparison to PBS-sensitized controls (Fig. 5A). Moreover, macrophages

388 and lymphocytes were increased at all time points (Fig. 5A). Interestingly, lymphocytes

17

389   and eosinophils continued to be detectable 28 days post challenge, but at lower levels.

390   Overall neutrophils decreased over time, but no significant differences were observed

391   between control and experimental groups at any time points (Fig. 5A). The inflammatory

392   response was also assessed by staining lung sections for H&E. Some cellular infiltrates

393   were observed in PBS-sensitized mice 2 and 7 days post challenge with W72310, while

394   robust inflammation, including eosinophils, was observed in animals sensitized and

395   challenged with W72310 at all time points (Fig. 5B). Furthermore, animals sensitized

396   and challenged with W72310 for all time points had detectable mucous cells in airways

397   as shown by PAS-stained lung sections (Fig. 5B, black arrows). At early time-points, 2

398   and 7 days after challenge, there were a large number of mucus-producing cells, which

399   persisted at lower levels at later time-points.

400   Total albumin in the BAL was measured to evaluate the extent of vascular

401   leakage and potential damage to the lungs in the airways. Quantification of albumin

402   showed significant increases in animals sensitized with W72310 and challenged 7 and

403   21 days compared to PBS-sensitized controls, indicating airway damage that resolved

404   by day 28 (Fig. 5C).

405   *Mice recall challenged with W72310 have increased airway inflammation and damage*

406   *in the lungs*: Major features of ABPA disease are periods of remission and exacerbation

407   (37). To determine if mice with persistent W72310 in the lungs were susceptible to a

408   recall response, mice were sensitized and challenged with either PBS or W72310 and

409   21 days after challenge all animals were recall challenged with either PBS or W72310

410   live conidia (Fig. 6A). BAL and lung suspension neutrophils and eosinophils were

411   significantly increased in the W72310 recall challenged group compared to PBS recall

18

412   challenged group (Fig. 6B). Serum IgE levels were increased 5-fold in mice sensitized

413   and challenged with W72310 at 21 days compared to PBS sensitized challenged mice,

414   as would be expected (based on results from the time course (Figs. 4D)) and BAL

415   albumin was measured in order to assess damage and leakage in the airways (Fig. 6C).

416   Total albumin levels were increased two-fold in the airways of mice sensitized,

417   challenged, and recall challenged with W72310 compared to both PBS controls. Th2

418   cytokines IL-4/IL-10 and Th1 cytokine IFNγ were significantly increased in BAL of mice

419   sensitized, challenged, and recall challenged with W72310 compared to PBS controls

420   (Fig. 6D). IL-17A cytokine levels were not detectable (data not shown). Collectively

421   these data demonstrate that W72310 persists for several weeks in a fungal-sensitized

422   murine lung and elicits strong inflammation, damage, mucus production, and an

423   exacerbation-like immune response.

424   *Comparison of W72310 and CEA10 whole genome sequences:* Given the clear immune

425   response differences to CEA10 and W72310, we wanted to address potential fungal

426   mediated mechanisms for these observations. As a first step toward understanding the

427   fungal contribution to these responses, whole genome sequencing of CEA10 and

428   W72310 was conducted. Sequencing and variant analysis revealed a total of 56,036

429   variants in W72310 that differed from the AF293 reference genome, compared to only

430   13,014 variants identified in CEA10. These variants included 2392 positions in W72310,

431   and 874 variants in CEA10 for which no allele could be determined (and which possibly

432   represent a deletion at that position when compared to AF293 reference genome). We

433   consequently identified 49,806 variants that were exclusive to W72310 and not shared

434   with CEA10 (18,088 excluding synonymous and intergenic variants), compared to only

19

435   8302 variants found in CEA10 but not present in W72310 (1922 excluding synonymous

436   and intergenic variants). W72310 also had a greater number of missense variants with a

437   total of 6486, compared to only 814 in CEA10. Given the differences observed between

438   W72310 and CEA10 in conidia viability, germination rate, and persistence in the lung,

439   we narrowed our focus to non-synonymous variants unique to W72310 (not present in

440   CEA10) occurring in genes involved in oxidative stress responses, cell wall biology,

441   melanin, and metabolism using reverse GO term mapping. Variants were identified in

442   20 unique oxidative stress response genes, 6 cell wall genes, and 6 melanin genes

443   (Table 1). Interestingly, no variants were identified in core metabolism genes. When

444   non-synonymous variants unique to W72310 were mapped onto putative allergen

445   genes, 184 SNPs and INDELS in 69 unique genes, with mutation load ranging from 1 to

446   21 variants per gene were found (Table 2). In order to corroborate differences observed

447   in oxidative stress resistance, mRFP-CEA10 and mRFP-W72310 strains were assayed

448   for susceptibility to oxidative stress inducing agents, hydrogen peroxide and menadione.

449   The percentage of viable CEA10 conidia (RFP$^+$) significantly reduced by 50% (hydrogen

450   peroxide) and 40% (menadione), respectively. In contrast, incubation of W72310 with

451   hydrogen peroxide and menadione only decreased the percentage of viable conidia by

452   less than 5% (Fig. 7A). Collectively these data show that W72310 conidia are less

453   susceptible to oxidative stress-induced death compared to CEA10 and this may

454   contribute to its persistent phenotype in the mouse lung. The allele(s) driving this

455   phenotype in W72310 conidia remain to be determined in future studies.

456

457

20

458 DISCUSSION

459   In the current study, we characterized a unique clinical strain of *A. fumigatus*

460 which persists in the murine lung and elicits an ABPA-like disease state. By identifying

461 and characterizing the W72310 strain, our studies demonstrated that an *A. fumigatus*

462 strain can be resistant to immune cell-mediated killing and that it can persist in the

463 murine lung as viable conidia while eliciting a strong IgE/inflammatory/damage

464 response. These data are important because they suggest *A. fumigatus* strains exist in

465 the population that can persist in mammalian airways and induce pathological immune

466 responses without robust fungal growth. Moreover, our data provide an opportunity to

467 uncover novel fungal contributions to allergic-like diseases due to the long-term

468 persistence of W72310 conidia in murine lungs.

469   We hypothesize that a key fungal mechanism for fungal persistence is enhanced

470 oxidative stress resistance of the W72310 conidia. Reactive Oxygen Species (ROS)

471 generated by NADPH-oxidases in neutrophils and macrophages are critical components

472 in host defense against *A. fumigatus* infection (25, 38). Intriguingly, our data

473 demonstrate that W72310 conidia are more resistant to both hydrogen peroxide and

474 menadione-induced death compared to CEA10 (Fig. 7). Moreover, neutrophils and

475 macrophages have reduced killing of W72310 conidia compared to CEA10 conidia (Fig.

476 1G). Genome sequencing revealed that W72310 has 20 oxidative stress response

477 genes with high impact SNPs (Table 1). Of particular interest perhaps the catalase

478 Afu6g03890/*catA* has 6 variants in W72310 and not CEA10 (Table 1). Previous studies

479 demonstrated that a catalase mutant generated in *A. fumigatus* was more sensitive to

480 hydrogen peroxide. Interestingly, its conidia did not have any difference in susceptibility

21

481 to immune cell mediated killing and had similar pathogenicity in mouse models of

482 aspergillosis compared to wild-type controls (39–41). Since there are 20 oxidative stress

483 response genes with variants in the W72310 strain, it seems likely that more than one

484 gene/mechanism is involved in its defense against ROS-induced killing. However, we

485 cannot rule out that novel alleles of genes like *catA* encode proteins with increased

486 activity.

487   Another fungal-centric striking observation from our studies is that W72310

488 persists in the mouse lung largely as viable conidia. Based on the histology at 21 days

489 post challenge (Fig. 4C), we observed that the majority of conidia appear to be

490 phagocytosed by large macrophage-like cells. Previous histological analyses of invasive

491 aspergillosis patients have also demonstrated the presence of multiple conidia per giant

492 cell (42), however, the viability of the fungus is not known. Case reports often show *A.*

493 *fumigatus* in the lung as germlings or hyphae by GMS stain (43), but it is not known

494 whether conidia, germlings, hyphae, or some combination contribute to ABPA and

495 fungal allergic disease pathogenesis. Given that W72310 has previously been shown to

496 have reduced germination rates in comparison to other strains (32, 33), another

497 explanation for its persistence is that remaining in its conidial form does not allow full

498 immune recognition of the fungus. Of note, W72310 elicited less of an inflammatory

499 response compared to CEA10 in an immune competent pulmonary challenge model

500 (Fig. 1E). LC3-associated phagocytosis has been shown to be critical in fungal killing

501 and is dependent on exposure of the fungal cell wall components, melanin and β-glucan

502 (44). Sequence analysis showed high impact SNPs in 6 cell wall genes and 6 melanin

503 genes which could potentially prevent full recognition and/or killing of the fungus (Table

22

504   1). Collectively, SNPs in melanin and cell wall stress genes may affect overall

505   germination and immune cell recognition of W72310 and SNPs in oxidative stress

506   response genes could affect overall viability of phagocytosed W72310 conidia. Rigorous

507   fungal genetic studies will be needed to determine specifically which gene(s) are

508   important overall for the persistent phenotype.

509   Despite a similar immunological response to sensitization between W72310 and

510   CEA10, select interferon-responsive genes were differentially expressed. CXCR3 was

511   not differentially expressed between W72310 and CEA10 (data not shown), however,

512   expression of its ligands, CXCL-9 and CXCL-10, was higher in W72310-sensitized

513   lungs compared to CEA10. CXCL9 and CXCL10, which have been shown to be induced

514   in other mouse models of asthma and *A. fumigatus*-induced inflammation (45–47),

515   activate Th1-type immune responses through CXCR3. Because CXCR3 is preferentially

516   expressed in Th1 cells, (48), this could indicate a potential role for the Th1 immune

517   response in the overall persistence observed from W72310. In both a mouse model of

518   severe asthma and in humans with severe asthma, CXCL-10 was shown to play a

519   critical role in corticosteroid resistance and Th1-mediated inflammation (49). However,

520   differences in the immune response at this time point could be either in response to the

521   different strains of fungi or different quantities of fungi since we observe significantly

522   more W72310 CFUs at this time point (Fig. 2C).

523   The results of our present study indicate that persistent conidial colonization in

524   the fungal-sensitized mouse lung causes many features of APBA-like disease (Figs 4-

525   6). Diagnosis of ABPA has proven to be challenging and it has long been postulated

526   that ABPA rates are under-represented due to a lack of consistency in diagnostic

23

527   methods (34). Elevated total and *A. fumigatus* specific IgE, *A. fumigatus* cutaneous

528   reactivity, bronchial asthma, airway eosinophilia, and bronchiectasis are the major

529   criteria utilized to diagnose APBA. Our data show increased airway eosinophilia, serum

530   IgE, and albumin in the BAL of mice up to 21 days after challenge with *A. fumigatus*,

531   indicating a pathogenic role for *A. fumigatus* long-term persistence. In other published

532   mouse models of ABPA, repeated inoculation is required for these phenotypes to be

533   maintained (45, 50). Further analysis of airway mechanics, host immunology and

534   changes in morphology will be needed to determine the extent of ABPA-disease like

535   pathogenesis in animals with a longer term W72310 infection.

536   Importantly, ABPA is primarily diagnosed in patients with Cystic Fibrosis, due to

537   an environment in the lung prone to long-term microbial colonization. Mouse models of

538   CF have also shown a strong role for *A. fumigatus* in CF disease pathogenesis. CFTR

539   KO and dF508 mice develop robust inflammatory, IL-4, and IgE (specifically in CD4+ T

540   cells) response to *A.f.* hyphal extract (51). Additionally, exposure of mice to *A. fumigatus*

541   conidia for 24h-72h causes increased inflammation, mucous production and BAL

542   inflammatory cytokine production in CFTR KO compared to WT mice (52) and

543   increased inflammasome activity was observed in CFTR KO mice in response to *A.*

544   *fumigatus* conidia exposure (53). Future experiments exposing genetically engineered

545   CF mice to W72310 could provide valuable insight into mechanisms of disease

546   pathogenesis and therapeutic efficacy. These types of studies could be especially

547   critical because the concept that strains of *A. fumigatus* can survive in the lung without

548   germinating but cause ABPA-like disease would significantly affect the types of

549   treatments a patient would receive, including antifungals. Moreover, identification of

24

550 specific fungal alleles that promote long term persistence may help diagnose chronic

551 infections in lieu of transient colonization that would help guide antifungal deployment in

552 these at-risk groups, such as CF patients.

564

565

566

567

568

569

570

571

572

573

574   FIGURES

575

Figure 1: *A. fumigatus* clinical isolate, W72310, persists longer in the murine lung and is

resistant to leukocyte-mediated death compared to common laboratory strain, CEA10.
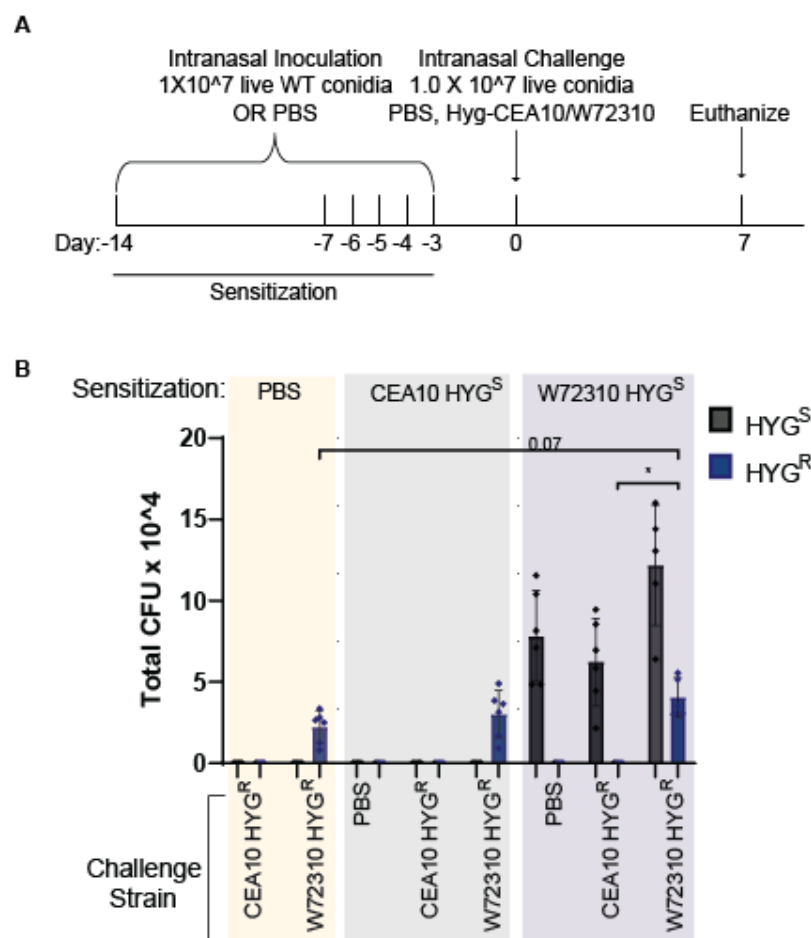
(A) C57Bl/6 mice were intranasally inoculated with 1X10^7 live CEA10 or W72310

conidia and euthanized after 7 days. Lungs were fixed in formalin and stained for fungi

(GMS stain, black). N=6-8 animals, scale bars=100um, 40X. **(B)** Lungs from parallel

581   experiments were assessed for total colony forming units (N=6-8 animals). C57Bl/6

582   mice were oropharyngeally inoculated with 3.0X10^7 AF633-stained mRFP-CEA10 or

583   mRFP-W72310 conidia for 36hrs. Lungs were analyzed by flow cytometry for **(C)** %

584   phagocytosis of conidia in immune cells (AF633$^+$/CD45$^+$), **(D)** % positive conidia

585   (AF633) in neutrophils and macrophages, and **(E)** total neutrophils

586   (CD45$^+$/Ly6G$^+$/CD11b$^+$) and macrophages (CD45$^+$/Ly6G$^-$/CD11b$^+$/CD64$^+$). **(F)** Viability

587   of conidia phagocytosed in neutrophils and macrophages was analyzed by flow

588   cytometry and **(G)** quantified. Representative micrographs were selected out of 6 mice

589   per group. Mann-Whitney single comparisons were used and NS P>0.05; * P$\leq$0.05; **

590   P$\leq$0.01; *** P$\leq$0.001.

591
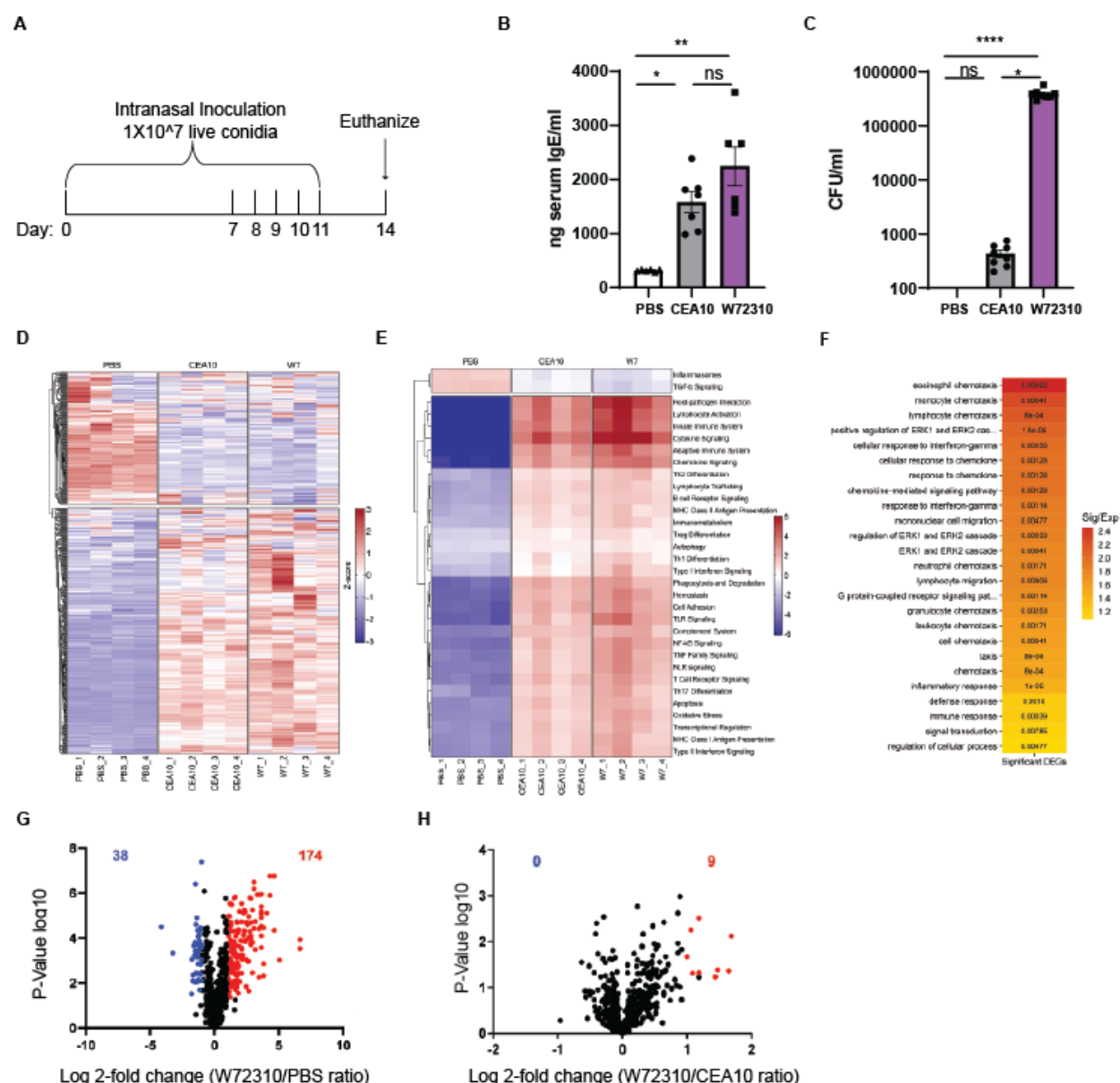
Figure 2: W72310-induced sensitization is similar to CEA10-induced sensitization in the murine lung. **(A)** Mice were inoculated with either PBS or 1X10^7 live W72310/CEA10 conidia on the indicated days and euthanized on day 14. **(B)** Total serum IgE was measured by ELISA on blood samples collected from animals. N=6-7 mice. **(C)** Total CFUs were measured in the lungs of mice. N=8 mice. Mann-Whitney with Dunn's multiple comparison were used and * P≤0.05; ** P≤0.01; *** P≤0.001; **** P≤0.0001.

598   **(D)** Total mRNA was extracted from the whole lung and gene expression was analyzed

599   by NanoString nCounter® Immunology panel. Downregulation (blue) or upregulation

600   (red) of individual replicates were represented by heat map, n=4 mice/group. **(E)**

601   Pathway signature of mice sensitized to either PBS, CEA10 or W72310. **(F)** Heatmap

602   showing the degree of enrichment and p-value for each GO-term enriched in increased

603   genes. The color of each tile indicates the log2 transformed degree of enrichment for a

604   given term within each gene set. The p-value is overlaid in text to show the significance

605   of each term. The terms on the y-axis are ordered according to decreasing degree of

606   enrichment from top to bottom. **(G)** Volcano plot showing the distribution of fold changes

607   in gene expression in W72310-treated mice compared to PBS: genes with absolute fold

608   changes ≤ 2 and with p value ≤ 0.05 (Student's T-test) are shown in blue and genes with

609   absolute fold changes ≥ 2 and with p value ≤ 0.05 (Student's T-test) are shown in red.

610   **(H)** Volcano plot showing the distribution of fold changes in gene expression in

611   W72310-treated mice compared to CEA10: genes with absolute fold changes ≥ 2 and

612   with p value ≤ 0.05 (Student's T-test) are shown in red.

29

613

Figure 3: W72310 accumulates in the mouse lung during sensitization. **(A)** C57Bl/6

mice were inoculated with either PBS or 1X10^7 live W72310/CEA10 conidia on the

indicated days (sensitization) and challenged on day 0 with either PBS, hyg-CEA10, or

hyg-W72310; animals were euthanized 7 days after challenge. **(B)** Lung homogenates

were spread on plates containing SAB alone or SAB plus hygromycin and quantified for

total CFU's. "Challenge" CFUs were identified as colonies grown on hygromycin plates

and "Sensitization" CFUs were calculated by subtracting hygromycin CFU values from

total CFU values (SAB alone plates). HYG^S=hygromycin sensitive and HYG^R=

hygromycin resistant. N= 6-12 mice per group. Mann-Whitney with Dunn's multiple

comparison were used and * $P \leq 0.05$.

624
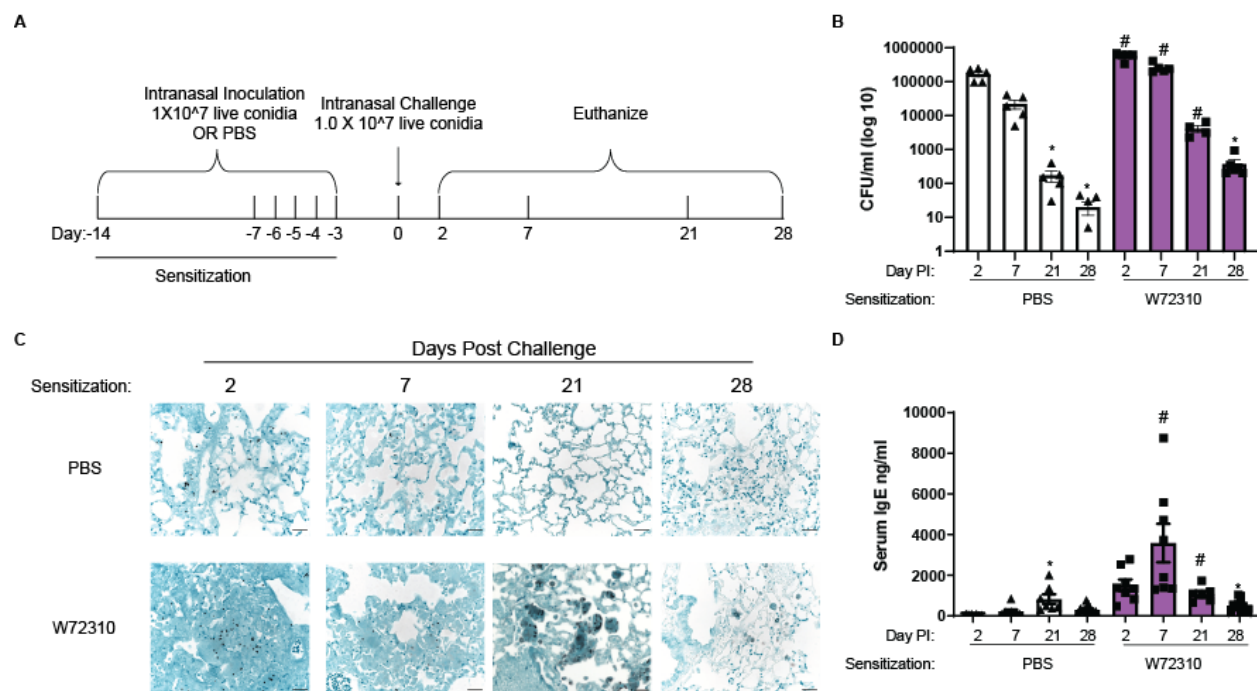
Figure 4: Sensitization and Challenge with W72310 causes increased fungal

persistence in the lung in association with increased serum IgE. (A) Schematic of

ABPA model protocol: C57Bl/6 mice were inoculated with either PBS or 1X10^7 live

W72310 conidia on the indicated days and challenged on day 0. Animals were

subsequently euthanized on days 2, 7, 21, and 28. (B) Colony Forming Units (CFUs)

were quantified from total lung homogenates at the indicated time points and

represented on a log scale. (C) Paraffin-embedded fixed lungs were stained for GMS

and images were captured at 40X, scale bar=100μm. (D) Total serum IgE was

measured by ELISA on blood samples collected from animals. (B and D) Kruskal Wallis

with Dunn's comparison to 2 day time point (within same sensitization protocol) *≤ 0.05;

Kruskal Wallis with Dunn's comparison to same time point (within different sensitization

protocol) #≤ 0.05. Data include 2 independent experiments and n=8-12 mice.
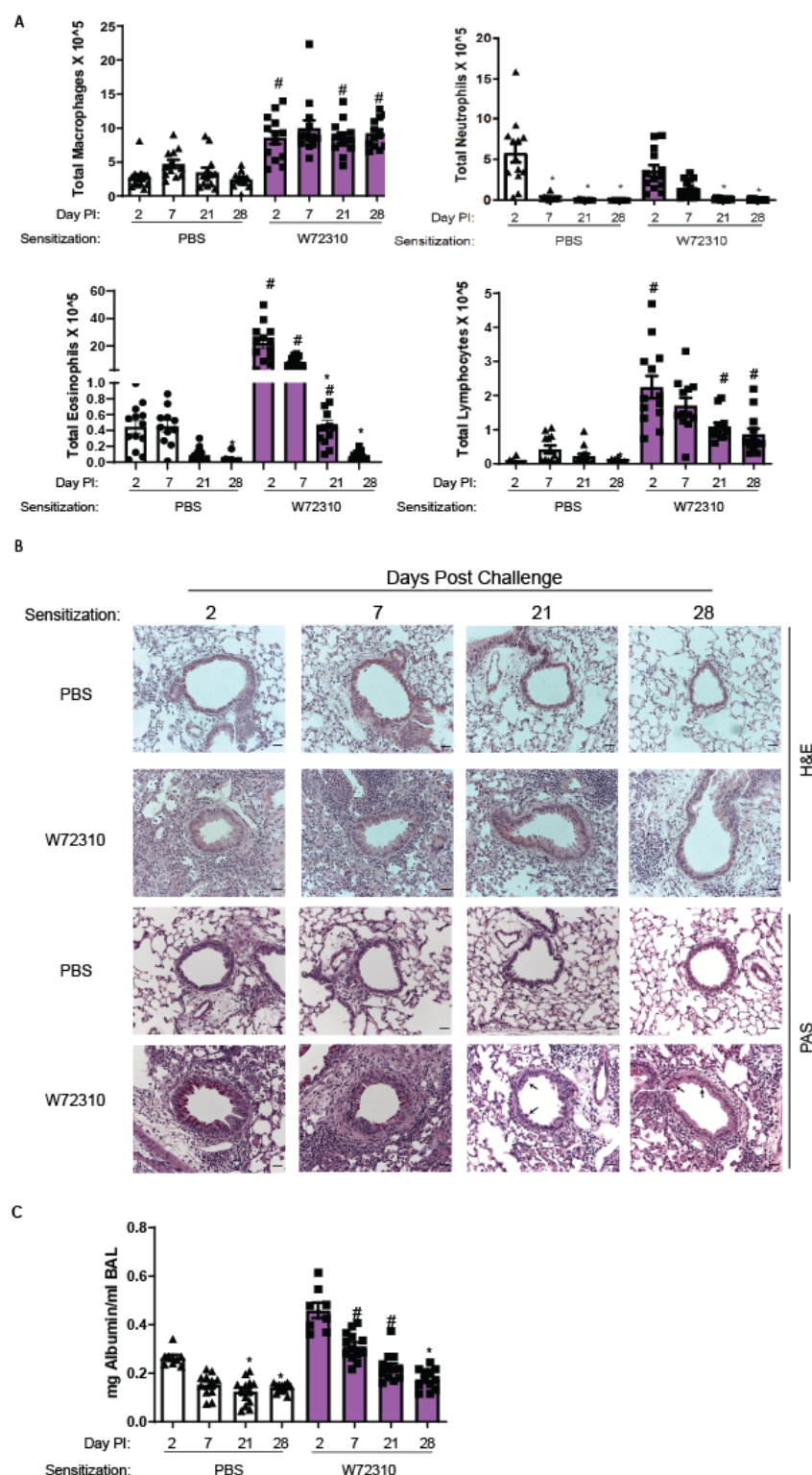
Figure 5: Sensitization and Challenge with W72310 causes increased pulmonary inflammation, leakage, and mucous cell metaplasia **(A)** Total BAL was quantified for

640   individual cell populations of macrophages, neutrophils, lymphocytes, and eosinophils.

641   **(B)** Paraffin-embedded fixed lungs were stained for H&E and PAS and images were

642   captured at 20X, scale bar=100μm. **(C)** BAL supernatant was analyzed for total

643   concentrations of albumin. (A and B) Kruskal Wallis with Dunn's comparison to 2 day

644   time point (within same sensitization protocol) *$\leq$ 0.05; Kruskal Wallis with Dunn's

645   comparison to same time point (within different sensitization protocol) #$\leq$ 0.05. Data

646   include 2 independent experiments and n=8-12 mice.
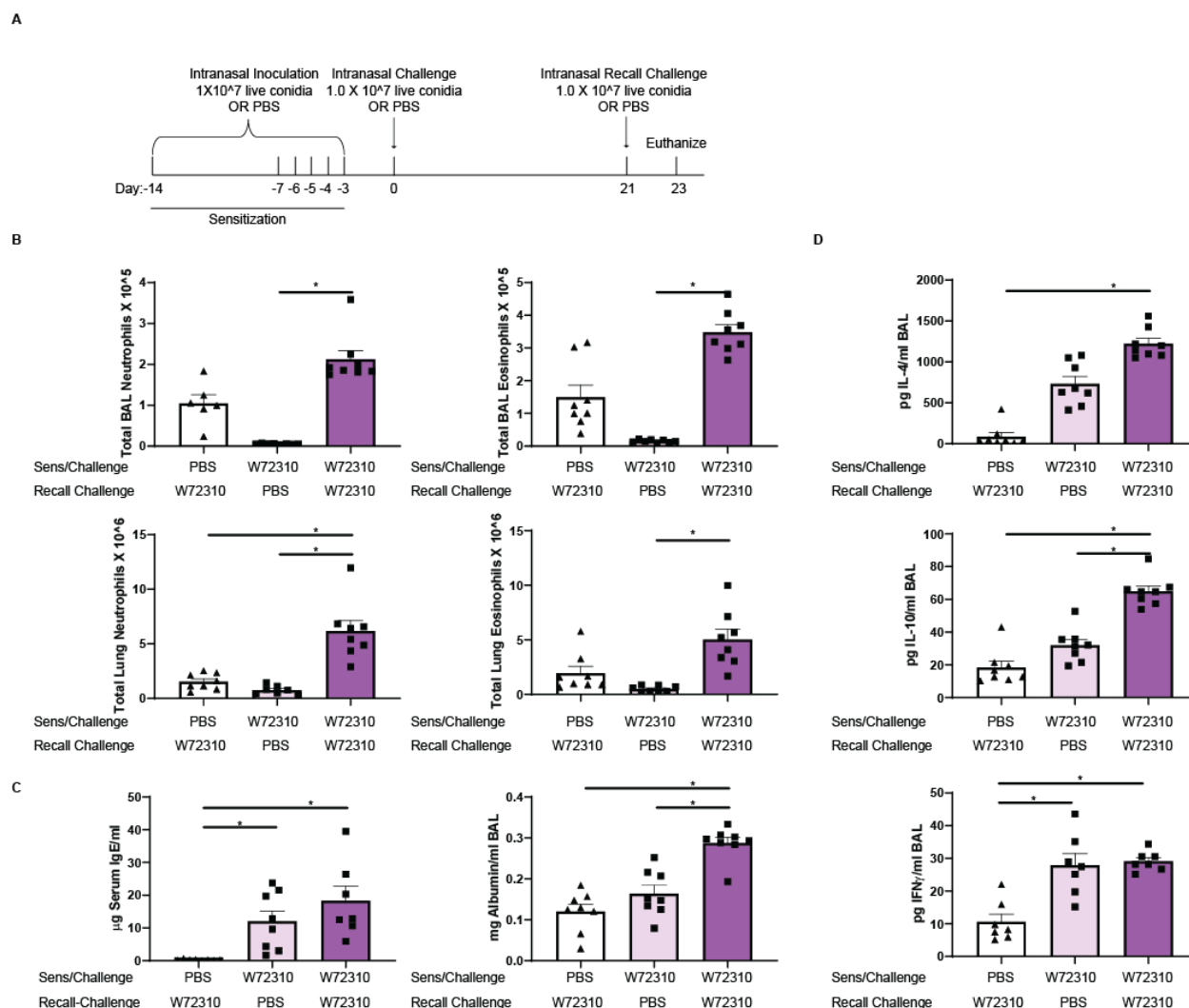
Figure 6: Sensitization and Challenge with W72310 and subsequent recall challenge causes increased tissue inflammation, damage, Th1/2, and IgE response. (A) Schematic of ABPA exacerbation protocol: C57Bl/6 mice were inoculated with either PBS or 1X10^7 live W72310 conidia on the indicated days (sensitization and challenge) and recall challenged 21 days after initial challenge. Animals were subsequently euthanized 48h later. (B) Neutrophils (CD45$^+$/SiglecF$^-$/Ly6G$^+$/CD11b$^{+)}$ and eosinophils (CD45$^+$/SiglecF$^+$/CD11c^{low}) were quantified by flow cytometry in BAL and lung suspensions. (C) Serum was isolated from mice and total IgE levels were quantified and

34

656   BAL supernatant was analyzed for total albumin. **(D)** BAL supernatant IL-4, IL-10 and

657   IFNγ were measured. Mann-Whitney with Dunn's multiple comparison were used and *

658   P$\leq$0.05.

659
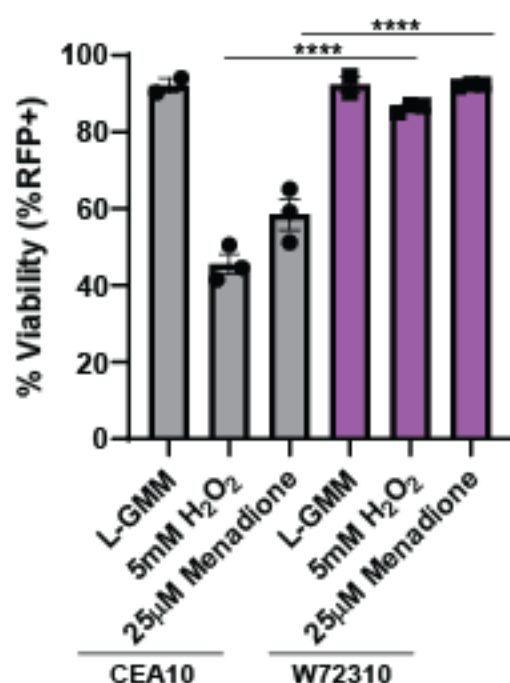
Figure 7: W72310 is more resistant to oxidative stress-induced death than CEA10. **(A)**

mRFP-CEA10 and mRFP-W72310 were incubated with either 25µM menadione or

5mM H_2O_2 for 6h and analyzed by flow cytometry for viability (%RFP$^+$). Data are

representative of 3 independent experiments with 3-4 technical replicates/experiment.

One way ANOVA with Tukey's multiple comparison were used and **** $P \leq 0.0001$.

665

666

667

668

669

670

Non-synonamous variants found in W7 relative to AF293, that are not found in CEA10

	Gene ID	# Exclusive Variants	Annotation
O2 stress	Afu2g01520	10	Ortholog(s) have role in ascospore formation, hyphal growth, response to oxidative stress, sporocarp development involved in sexual reproduction
	Afu3g10530	6	Putative protein serine/threonine kinase
	Afu6g03890	6	Spore-specific catalase
	Afu2g04680	5	Protein serine/threonine kinase
	Afu4g10770	5	Psi-producing oxygenase A
	Afu5g11820	5	Ortholog(s) have cytosol, nucleus localization
	Afu6g12522	5	Putative transcription factor and response regulator of a two-component signal transduction system
	Afu2g00200	4	Ortholog(s) have catalase activity
	Afu1g13600	3	Ortholog(s) have cyclin-dependent protein kinase activating kinase activity, cyclin-dependent protein serine/threonine kinase regulator activity, protein serine/threonine kinase activity
	Afu3g12670	3	Putative serine/threonine protein kinase
	Afu4g09110	3	Putative cytochrome c peroxidase
	Afu2g01700	2	Ortholog(s) have AMP-activated protein kinase activity, ARF guanyl-nucleotide exchange factor activity
	Afu3g02270*	2	Mycelial catalase
	Afu4g00180	2	Fatty acid 8,11-diol synthase
	Afu7g03720	2	Ortholog(s) have RNA polymerase II carboxy-terminal domain kinase activity, cyclin-dependent protein kinase activating kinase activity, cyclin-dependent protein serine/threonine kinase activity
	Afu1g01980	1	Ortholog(s) have role in hyphal growth, response to cold, response to heat, response to oxidative stress, response to salt stress, sporocarp development involved in sexual reproduction
	Afu1g05930	1	Ortholog(s) have protein serine/threonine kinase activity
	Afu3g12120	1	Putative fatty acid oxygenase
	Afu5g08580	1	Putative alpha-1,6-mannosyltransferase that initiates the linkage of the N-glycan outer chain
	Afu5g09240	1	Cu/Zn superoxide dismutase
Cell Wall	Afu1g13670	5	Conidial cell wall protein A
	Afu6g08510	5	Putative cell wall biosynthesis protein
	Afu3g07650	4	Has domain(s) with predicted pectinesterase activity, role in cell wall modification and cell wall localization
	Afu2g03120	2	Putative cell wall glucanase
	Afu4g03240*	2	Putative cell wall galactomannoprotein
	Afu8g06880	2	Ortholog(s) have pectinesterase activity and role in pectin catabolic process
Melanin	Afu2g04200	9	4-hydroxyphenylpyruvate dioxygenase involved in the L-tyrosine degradation pathway
	Afu1g16590	7	Putative C2H2 transcription factor
	Afu1g15440	4	Putative alpha(1-3) glucan synthase
	Afu2g17550	1	Heptaketide hydrolyase ayg1
	Afu2g17560	1	1,3,6,8-tetrahydroxynaphthalene reductase arp2
	Afu2g17600	1	Conidial pigment polyketide synthase alb1

Non-synonamous variants found in W7 relative to AF293, that are not found in CEA10

	Gene ID	# Exclusive Variants	Annotation
	Afu1g02980	21	Putative 6-phosphogluconolactonase
	Afu7g05740	10	Putative NAD-dependent malate dehydrogenase
	Afu5g11320	9	Allergen Asp f 29
	Afu5g04170	6	Heat shock protein
	Afu1g14560	5	Putative 1,2-alpha-mannosidase
	Afu2g01010	5	Putative myo-inositol-phosphate synthase
	Afu2g01170	5	1,3-beta-glucanosyltransferase with a role in elongation of 1,3-beta-glucan chains
	Afu3g11690	5	Putative class II fructose-bisphosphate aldolase
	Afu1g09470	4	Putative class V aminotransferase
	Afu1g09670	4	Putative HLH transcription factor
	Afu2g13530	4	Putative translation elongation factor EF-2 subunit
	Afu3g00590	4	Asp-hemolysin
	Afu4g01290	4	Glycosyl hydrolase family 75 chitosanase
	Afu6g10300	4	Allergen Asp f 28
	Afu1g14570	3	Putative phosphoribosyl-AMP cyclohydrolase
	Afu2g03830	3	Allergen Asp f 4
	Afu2g09960	3	Putative mitochondrial Hsp70 chaperone
	Afu3g01110	3	Putative GMP synthase ([glutamine-hydrolyzing)
	Afu4g10130	3	Ortholog(s) have alpha-amylase activity and role in carbohydrate catabolic process
	Afu4g11720	3	Putative phosphatidyl synthase
	Afu5g09580	3	Conidial hydrophobin
	Afu6g04920	3	Putative NAD-dependent formate dehydrogenase
	Afu6g10660	3	Putative ATP citrate lyase subunit
	Afu7g05720	3	Pyruvate dehydrogenase complex, dihydrolipoamide acetyltransferase component
	Afu1g04130	2	FG-GAP repeat protein
	Afu2g10100	2	Allergen Asp f 8
	Afu2g11150	2	Putative secretory-pathway GDP dissociation inhibitor
	Afu2g11260	2	Putative 3-isopropylmalate dehydratase with a predicted role in nitrogen metabolism
	Afu2g16820	2	Putative curved DNA-binding protein
	Afu3g00600	2	Ortholog of Aspergillus fumigatus A1163 : AFUB_047840
	Afu3g02270*	2	Mycelial catalase
	Afu3g09320	2	Serine hydroxymethyltransferase
	Afu4g03240*	2	Putative cell wall galactomannoprotein
Allergen	Afu4g06670	2	Allergen Asp f 7
	Afu4g10460	2	Homocitrate synthase, essential enzyme of the alpha-aminoadipate pathway of lysine biosynthesis
	Afu5g05540	2	Putative nucleosome assembly protein
	Afu5g09210	2	Autophagic (vacuolar) serine protease
	Afu5g13300	2	Putative extracellular aspartic endopeptidase
	Afu6g02230	2	Putative glucokinase
	Afu6g02280	2	Allergen Asp f 3
	Afu6g09690	2	Glutathione S-transferase gliG
	Afu6g09740	2	Thioredoxin reductase gliT
	Afu8g07080	2	Putative secreted metalloprotease
	Afu1g02820	1	Putative NADH-quinone oxidoreductase
	Afu1g06830	1	Putative 60s acidic ribosomal protein superfamily member
	Afu1g07440	1	Molecular chaperone
	Afu1g08980	1	UPF0160 domain protein
	Afu1g10630	1	Putative S-adenosylmethionine synthetase
	Afu1g11460	1	Putative 1,3-beta-glucanosyltransferase
	Afu2g00690	1	Ortholog(s) have glucan 1,4-alpha-glucosidase activity, role in polysaccharide metabolic process and Golgi apparatus, endoplasmic reticulum, prospore membrane localization
	Afu2g06150	1	Putative protein disulfide isomerase
	Afu2g12630	1	Allergen Asp f 13
	Afu2g13250	1	Putative bifunctional tryptophan synthase
	Afu2g15430	1	Sorbitol/xylulose reductase
	Afu3g03060	1	Allergen Asp f 34
	Afu3g07430	1	Putative peptidyl-prolyl cis-trans isomerase
	Afu3g10460	1	Putative nuclear transport factor
	Afu3g11300	1	Putative proteasome component
	Afu3g11400	1	Aspartic acid endopeptidase
	Afu4g00610	1	Putative aryl-alcohol dehydrogenase
	Afu4g07410	1	Has domain(s) with predicted catalytic activity
	Afu4g07690	1	Putative phosphoribosylaminoimidazole-carboxamide formyltransferase/IMP cyclohydrolase
	Afu4g08720	1	Putative secreted phospholipase B
	Afu5g06390	1	Putative adenosine kinase
	Afu5g10550	1	ATP synthase F1, beta subunit
	Afu6g06770	1	Putative enolase
	Afu6g11330	1	Ortholog(s) have thiamine phosphate phosphatase activity and role in dephosphorylation, thiamine biosynthetic process
	Afu6g12930	1	Mitochondrial aconitate hydratase
	Afu8g05020	1	Putative secreted N-acetylhexosaminidase

673

674
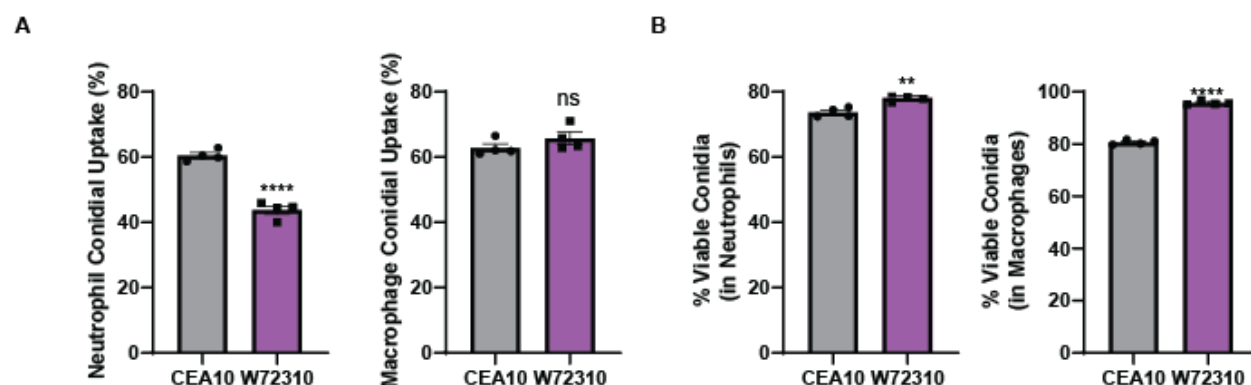
Supplemental Figure 1: W72310 is more resistant to bone marrow cell-induced death than CEA10. **(A)** AF633-stained mRFP-CEA10 and mRFP-W72310 live conidia were incubated with murine bone marrow for 16 hours and analyzed by flow cytometry for % positive conidia (AF633) in neutrophils and macrophages and **(B)** % viable conidia (AF633$^+$/RFP$^+$) in neutrophils and macrophages. Data include 3 independent experiments with 3-4 replicates per experiment. Mann-Whitney with Dunn's multiple comparison were used and NS>0.05; * P$\leq$0.05; ** P$\leq$0.01; *** P$\leq$0.001; **** P$\leq$0.0001.

682   REFERENCES:

683   1.   Pashley CH. 2014. Fungal Culture and Sensitisation in Asthma, Cystic Fibrosis

684   and Chronic Obstructive Pulmonary Disorder: What Does It Tell Us?

685   Mycopathologia 178:457–463.

686   2.   Haase G, Skopnik H, Groten T, Kusenbach G, Posselt HG. 1991. Long-term

687   fungal cultures from sputum of patients with cystic fibrosis: Langzeitpilzkulturen

688   von Sputen bei Patienten mit zystischer Fibrose. Mycoses 34:373–376.

689   3.   Rapaka RR, Kolls JK. 2009. Pathogenesis of allergic bronchopulmonary

690   aspergillosis in cystic fibrosis: current understanding and future directions. Med

691   Mycol 47 Suppl 1:S331-7.

692   4.   Saunders R V., Modha DE, Claydon A, Gaillard EA. 2016. Chronic *Aspergillus*

693   *fumigatus* colonization of the pediatric cystic fibrosis airway is common and may

694   be associated with a more rapid decline in lung function. Med Mycol 54:537–543.

695   5.   Stevens DA, Moss RB, Kurup VP, Knutsen AP, Greenberger P, Judson MA,

696   Denning DW, Crameri R, Brody AS, Light M, Skov M, Maish W, Mastella G,

697   Participants in the Cystic Fibrosis Foundation Consensus Conference. 2003.

698   Allergic Bronchopulmonary Aspergillosis in Cystic Fibrosis—State of the Art:

699   Cystic Fibrosis Foundation Consensus Conference. Clin Infect Dis 37:S225–

700   S264.

701   6.   King J, Brunel SF, Warris A. 2016. Aspergillus infections in cystic fibrosis. J Infect

702   72:S50–S55.

703   7.   Chotirmall SH, McElvaney NG. 2014. Fungi in the cystic fibrosis lung: Bystanders

704   or pathogens? Int J Biochem Cell Biol 52:161–173.

705   8.   Kauffman HF. 2003. Immunopathogenesis of allergic bronchopulmonary

706   aspergillosis and airway remodeling. Front Biosci 8:e190-6.

707   9.   Hayes D, Murphy BS, Lynch JE, Feola DJ. 2010. Aerosolized amphotericin for the

708   treatment of allergic bronchopulmonary aspergillosis. Pediatr Pulmonol 45:1145–

709   8.

710   10. Wark P. 2004. Pathogenesis of allergic bronchopulmonary aspergillosis and an

711   evidence-based review of azoles in treatment. Respir Med 98:915–23.

712   11. Urb M, Snarr BD, Wojewodka G, Lehoux M, Lee MJ, Ralph B, Divangahi M, King

713   IL, McGovern TK, Martin JG, Fraser R, Radzioch D, Sheppard DC. 2015.

714   Evolution of the Immune Response to Chronic Airway Colonization with

715   Aspergillus fumigatus Hyphae. Infect Immun 83:3590–3600.

716   12. Nawada R, Amitani R, Tanaka E, Niimi A, Suzuki K, Murayama T, Kuze F. 1996.

717   Murine model of invasive pulmonary aspergillosis following an earlier stage,

718   noninvasive Aspergillus infection. J Clin Microbiol 34:1433–1439.

719   13. Hogaboam CM, Gallinat CS, Taub DD, Strieter RM, Kunkel SL, Lukacs NW.

720   1999. Immunomodulatory role of C10 chemokine in a murine model of allergic

721   bronchopulmonary aspergillosis. J Immunol 162:6071–9.

722   14. Murdock BJ, Shreiner AB, McDonald RA, Osterholzer JJ, White ES, Toews GB,

723   Huffnagle GB. 2011. Coevolution of T_H1, T_H2, and T_H17 Responses during

41

724   Repeated Pulmonary Exposure to *Aspergillus fumigatus* Conidia. Infect Immun

725   79:125–135.

726   15.   Kosmidis C, Denning DW. 2015. The clinical spectrum of pulmonary aspergillosis.

727   Thorax 70:270–277.

728   16.   Paugam A, Baixench M-T, Demazes-Dufeu N, Burgel P-R, Sauter E, Kanaan R,

729   Dusser D, Dupouy-Camet J, Hubert D. 2010. Characteristics and consequences

730   of airway colonization by filamentous fungi in 201 adult patients with cystic fibrosis

731   in France. Med Mycol 48:S32–S36.

732   17.   Chen KTK. 1993. Cytology of allergic bronchopulmonary aspergillosis. Diagn

733   Cytopathol 9:82–85.

734   18.   Chetty A. 2003. Pathology of allergic bronchopulmonary aspergillosis. Front

735   Biosci. Front Biosci.

736   19.   Grahl N, Puttikamonkul S, Macdonald JM, Gamcsik MP, Ngo LY, Hohl TM,

737   Cramer RA. 2011. In vivo Hypoxia and a Fungal Alcohol Dehydrogenase

738   Influence the Pathogenesis of Invasive Pulmonary Aspergillosis. PLoS Pathog

739   7:e1002145.

740   20.   Kowalski CH, Kerkaert JD, Liu K-W, Bond MC, Hartmann R, Nadell CD, Stajich

741   JE, Cramer RA. 2019. Fungal biofilm morphology impacts hypoxia fitness and

742   disease progression. Nat Microbiol 1–12.

743   21.   Huang DW, Sherman BT, Lempicki RA. 2009. Bioinformatics enrichment tools:

744   Paths toward the comprehensive functional analysis of large gene lists. Nucleic

745   Acids Res 37:1–13.

746   22.   Huang DW, Sherman BT, Tan Q, Kir J, Liu D, Bryant D, Guo Y, Stephens R,

747   Baseler MW, Lane HC, Lempicki RA. 2007. DAVID Bioinformatics Resources:

748   Expanded annotation database and novel algorithms to better extract biology from

749   large gene lists. Nucleic Acids Res 35.

750   23.   Alexa A, Rahnenführer J, Lengauer T. 2006. Improved scoring of functional

751   groups from gene expression data by decorrelating GO graph structure.

752   Bioinformatics 22:1600–1607.

753   24.   Gu Z, Eils R, Schlesner M. 2016. Complex heatmaps reveal patterns and

754   correlations in multidimensional genomic data. Bioinformatics 32:2847–2849.

755   25.   Shlezinger N, Irmer H, Dhingra S, Beattie SR, Cramer RA, Braus GH, Sharon A,

756   Hohl TM. 2017. Sterilizing immunity in the lung relies on targeting fungal

757   apoptosis-like programmed cell death. Science (80-) 357:1037–1041.

758   26.   Jhingran A, Mar KB, Kumasaka DK, Knoblaugh SE, Ngo LY, Segal BH, Iwakura

759   Y, Lowell CA, Hamerman JA, Lin X, Hohl TM. 2012. Tracing conidial fate and

760   measuring host cell antifungal activity using a reporter of microbial viability in the

761   lung. Cell Rep 2:1762–73.

762   27.   Griffiths LJ, Anyim M, Doffman SR, Wilks M, Millar MR, Agrawal SG. 2006.

763   Comparison of DNA extraction methods for Aspergillus fumigatus using real-time

764   PCR. J Med Microbiol 55:1187–1191.

765   28.   Stajich JE, Harris T, Brunk BP, Brestelli J, Fischer S, Harb OS, Kissinger JC, Li

766   W, Nayak V, Pinney DF, Stoeckert CJ, Roos DS. 2012. FungiDB: An integrated

767   functional genomics database for fungi. Nucleic Acids Res 40.

768   29.   Basenko EY, Pulman JA, Shanmugasundram A, Harb OS, Crouch K, Starns D,

769   Warrenfeltz S, Aurrecoechea C, Stoeckert CJ, Kissinger JC, Roos DS, Hertz-

770   Fowler C. 2018. FungiDB: An integrated bioinformatic resource for fungi and

771   oomycetes. J Fungi 4.

772   30.   Li H, Wren J. 2014. Toward better understanding of artifacts in variant calling from

773   high-coverage samples. Bioinformatics. Oxford University Press.

774   31.   Stajich, Jason E. Lofgren LA. 2020. stajichlab/W72310: W72310 variant pipeline.

775   https://zenodo.org/record/4116457#.X8k75KpKgWo

776   32.   Kowalski CH, Beattie SR, Fuller KK, McGurk EA, Tang Y-W, Hohl TM, Obar JJ,

777   Cramer RA, Jr. 2016. Heterogeneity among Isolates Reveals that Fitness in Low

778   Oxygen Correlates with Aspergillus fumigatus Virulence. MBio 7.

779   33.   Caffrey-Carr AK, Kowalski CH, Beattie SR, Blaseg NA, Upshaw CR,

780   Thammahong A, Lust HE, Tang Y-W, Hohl TM, Cramer RA, Obar JJ. 2017.

781   Interleukin 1α Is Critical for Resistance against Highly Virulent Aspergillus

782   fumigatus Isolates. Infect Immun 85.

783   34.   Patel AR, Patel AR, Singh S, Singh S, Khawaja I. 2019. Diagnosing Allergic

784   Bronchopulmonary Aspergillosis: A Review. Cureus 11:e4550.

785   35.   Fukahori S, Matsuse H, Tsuchida T, Kawano T, Nishino T, Fukushima C, Kohno

786   S. 2014. Clearance of Aspergillus fumigatus is impaired in the airway in allergic

787   inflammation. Ann Allergy, Asthma Immunol 113:180–186.

788   36.   Keown K, Abbott S, Kuzeljevic B, Rayment JH, Chilvers MA, Yang CL. 2019. An

789   investigation into biomarkers for the diagnosis of ABPA and aspergillus disease in

790   cystic fibrosis. Pediatr Pulmonol 54:1787–1793.

791   37.   Agarwal R, Chakrabarti A, Shah A, Gupta D, Meis JF, Guleria R, Moss R,

792   Denning DW, ABPA complicating asthma ISHAM working group. 2013. Allergic

793   bronchopulmonary aspergillosis: review of literature and proposal of new

794   diagnostic and classification criteria. Clin Exp Allergy 43:850–873.

795   38.   Boyle KB, Stephens LR, Hawkins PT. 2012. Activation of the neutrophil NADPH

796   oxidase by Aspergillus fumigatus. Ann N Y Acad Sci 1273:68–73.

797   39.   Paris S, Wysong D, Debeaupuis JP, Shibuya K, Philippe B, Diamond RD, Latgé

798   JP. 2003. Catalases of Aspergillus fumigatus. Infect Immun 71:3551–3562.

799   40.   Calera JA, Paris S, Monod M, Hamilton AJ, Debeaupuis JP, Diaquin M, López-

800   Medrano R, Leal F, Latgé JP. 1997. Cloning and disruption of the antigenic

801   catalase gene of Aspergillus fumigatus. Infect Immun 65:4718–4724.

802   41.   Lessing F, Kniemeyer O, Wozniok I, Loeffler J, Kurzai O, Haertl A, Brakhage AA.

803   2007. The Aspergillus fumigatus transcriptional regulator AfYap1 represents the

804   major regulator for defense against reactive oxygen intermediates but is

805   dispensable for pathogenicity in an intranasal mouse infection model. Eukaryot

806   Cell 6:2290–2302.

807   42.   Milroy CM, Blanshard JD, Lucas S, Michaels L. 1989. Aspergillosis of the nose

45

808   and paranasal sinuses. J Clin Pathol 42:123–127.

809   43.   Lourdes Ylagan SP. 2014. Allergic Bronchopulmonary Aspergillosis: A Diagnostic

810   Challenge. J Cytol Histol s4.

811   44.   Akoumianaki T, Kyrmizi I, Valsecchi I, Gresnigt MS, Samonis G, Drakos E,

812   Boumpas D, Muszkieta L, Prevost MC, Kontoyiannis DP, Chavakis T, Netea MG,

813   Van De Veerdonk FL, Brakhage AA, El-Benna J, Beauvais A, Latge JP, Chamilos

814   G. 2016. Aspergillus Cell Wall Melanin Blocks LC3-Associated Phagocytosis to

815   Promote Pathogenicity. Cell Host Microbe 19:79–90.

816   45.   Ramaprakash H, Shibata T, Duffy KE, Ismailoglu UB, Bredernitz RM, Moreira AP,

817   Coelho AL, Das AM, Fursov N, Chupp GL, Hogaboam CM. 2011. Targeting ST2L

818   potentiates CpG-mediated therapeutic effects in a chronic fungal asthma model.

819   Am J Pathol 179:104–115.

820   46.   Schuh JM, Blease K, Hogaboam CM. 2002. CXCR2 is necessary for the

821   development and persistence of chronic fungal asthma in mice. J Immunol

822   168:1447–56.

823   47.   Su Y-C, Rolph MS, Hansbro NG, Mackay CR, Sewell WA. 2008. Granulocyte-

824   macrophage colony-stimulating factor is required for bronchial eosinophilia in a

825   murine model of allergic airway inflammation. J Immunol 180:2600–7.

826   48.   Bonecchi R, Bianchi G, Bordignon PP, D'Ambrosio D, Lang R, Borsatti A, Sozzani

827   S, Allavena P, Gray PA, Mantovani A, Sinigaglia F. 1998. Differential Expression

828   of Chemokine Receptors and Chemotactic Responsiveness of Type 1 T Helper

829   Cells (Th1s) and Th2s. J Exp Med 187:129–134.

830 49. Gauthier M, Chakraborty K, Oriss TB, Raundhal M, Das S, Chen J, Huff R, Sinha
831   A, Fajt M, Ray P, Wenzel SE, Ray A. 2017. Severe asthma in humans and mouse
832   model suggests a CXCL10 signature underlies corticosteroid-resistant Th1 bias.
833   JCI insight 2.

834 50. Hogaboam CM, Blease K, Mehrad B, Steinhauser ML, Standiford TJ, Kunkel SL,
835   Lukacs NW. 2000. Animal model: Chronic airway hyperreactivity, goblet cell
836   hyperplasia, and peribronchial fibrosis during allergic airway disease induced by
837   Aspergillus fumigatus. Am J Pathol 156:723–732.

838 51. Allard JB, Poynter ME, Marr KA, Cohn L, Rincon M, Whittaker LA. 2006.
839   Aspergillus fumigatus generates an enhanced Th2-biased immune response in
840   mice with defective cystic fibrosis transmembrane conductance regulator. J
841   Immunol 177:5186–94.

842 52. Chaudhary N, Datta K, Askin FB, Staab JF, Marr KA. 2012. Cystic Fibrosis
843   Transmembrane Conductance Regulator Regulates Epithelial Cell Response to
844   *Aspergillus* and Resultant Pulmonary Inflammation. Am J Respir Crit Care Med
845   185:301–310.

846 53. Iannitti RG, Napolioni V, Oikonomou V, De Luca A, Galosi C, Pariano M, Massi-
847   Benedetti C, Borghi M, Puccetti M, Lucidi V, Colombo C, Fiscarelli E, Lass-Flörl
848   C, Majo F, Cariani L, Russo M, Porcaro L, Ricciotti G, Ellemunter H, Ratclif L, De
849   Benedictis FM, Talesa VN, Dinarello CA, van de Veerdonk FL, Romani L. 2016.
850   IL-1 receptor antagonist ameliorates inflammasome-dependent inflammation in
851   murine and human cystic fibrosis. Nat Commun 7:10791.

852